Official Dental Journal of Suez Canal University
DENTAL SCIENCE Updates
Print ISSN 2636-3836
Online ISSN 2636-3844
www.dsujournals.ekb.eg
DSU — Vol. 6, No. 2, September (2025) — PP. 369:378

THE PUTATIVE REGENERATIVE CAPABILITY OF CELASTROL AND ITS NANOEMULSION ON OSTEOPOROTIC RATS EXPERIMENTALLY INDUCED BY OVARIECTOMY

Laila Fekry Elshahed[1], Doaa Ahmad Labah [2], Tamer Hassan[3], Rasha Mohamed Taha [4], Elham Fathy Mahmoud [5]

DOI: 10.21608/dsu.2025.362654.1289
Manuscript ID: DSU-2502-1289

KEYWORDS

Bone turnover markers, Celastrol, Nanoemulsion, Osteoporosis, Ovariectomy

- E-mail address: Lailaelshahed20@gmail.com

1. Assistant lecturer Oral Biology Department, Faculty of Dentistry, Zagazig University, Zagazig, Egypt
2. Professor of Oral Biology, Faculty of Dentistry, Zagazig University, Zagazig, Egypt
3. Lecturer at Pharmaceutics and Industrial Pharmacy Department, Faculty of Pharmacy, Suez Canal University, Ismailia, Egypt
4. Professor of Oral, Faculty of Dentistry, Suez Canal University, Ismailia, Egypt
5. Professor of Oral, Faculty of Dentistry, Suez Canal University, Ismailia, Egypt

ABSTRACT

Introduction: Postmenopausal osteoporosis (PMOP) is the most common bone disease in the developed world with serious public health concerns. Celastrol (CEL) has been voted as one of the top five promising natural medicine molecules which may help in PMOP management. Celastrol nanoemulsion (CTL-NE) was proved to improve the oral bioavailability, therapeutic effects of CTL. **Aim of the study:** To detect and compare the effect of CTL and CTL-NE on mandibular bone architecture and bone turnover markers (BTMs) in ovariectomized (OVX) rats as a model of PMOP. **Materials and Methods:** Two groups of sixty female rats; the OVX group and the sham group, were assigned at random. The rats in each group were further separated into three equal subgroups sixty days after OVX and sham operations. The rats in subgroup 1 were not given any treatment, those in subgroup 2 were given CTL, and those in subgroup 3 were given CTL-NE for four weeks. At the end of the experiment, blood samples were collected for biochemical analysis of bone turnover markers (BTMs), then the rats were euthanized, and their lower jaws were prepared for light microscope (LM). **Results:** Histological examination of OVX rats mandibular bone revealed compromised bone architecture and significant increase in BTMs compared with the normal sham ones. Interestingly OVX group showed notable improvement in bone microstructure and marked decrease in BTMs upon celastrol administration, however, the superior improvement was achieved in CTL-NE treated rats and these results were confirmed histologically and biochemically. **Conclusion:** Systemic administration of CTL and CTL-NE may be effective therapy for treatment of poor bone quality in OVX induced osteoporosis, with privilege to CTL-NE therapy.

INTRODUCTION

Osteoporosis is a skeletal-metabolic disease characterized by a decline in bone mineral density and disturbance of the bone microarchitecture. About 200 million people worldwide suffer from osteoporosis, including 34% of women over 50 and it is termed postmenopausal osteoporosis "PMOP", which is caused mainly by estrogen deficiency [(1)].

The clinical consequences of this systemic disorder mainly include an increased risk of bone fractures. Poor bone quality associated with PMOP seriously complicates the healing process. There is an urgent need to develop novel strategies for prevention and treatment of

osteoporosis-induced fractures which is the most serious complication of PMOP as they are linked to increased morbidity and death as well as a significant economic burden [2].

Numerous medications for treating osteoporosis have been studied and they are available in the market. Osteoporosis can be effectively treated and prevented with traditional anti-osteoporotic medications. However, because of their numerous negative effects, many women turn to herbal preparations as an alternative form of treatment. Traditional herbal medicine has recently drawn more attention since it contains many bioactive components that await discovery and research [3].

The "thunder god vine" is the common name for Tripterygium wilfordii. In China, it has long been used to treat autoimmune conditions such type 1 diabetes, Crohn's disease, and rheumatoid arthritis. Triterpenoids and alkaloids, which are mostly taken from the plant's root pulp, are among the phytochemicals that are abundant in the plant. Celastrol (CTL) is the most prevalent and promising bioactive molecule among these phytochemicals [4].

Over the past 20 years, CTL, also referred to as tripterine, has become more significant because of its strong anti-inflammatory, anti-cancer, neuroprotective, and antioxidant properties. Nevertheless, despite its potency, its clinical translation is hindered by two primary drawbacks: its narrow therapeutic index, which results in substantial systemic toxicity, and its poor water solubility, which restricts its bioavailability at 25°C (0.044 mg/ml) [5].

Numerous medication delivery strategies have been studied to address the toxicity concerns while maintaining the intended therapeutic efficacy. Because of its smaller size, targeting potential, and improved solubility and permeability—two factors that are beneficial in boosting the bioavailability of CTL—nanoparticulate drug delivery systems and nanoformulations of CTL have been highlighted as a promising approach [6].

Nanoemulsions are a type of nanotechnology. Fine oil-in-water dispersions with droplets ranging in size from 100 to 600 nm make up nanoemulsions. It was demonstrated that CTL-NE might enhance CTL's oral bioavailability, therapeutic benefits, and tissue targeting capacity [7].

MATERIALS AND METHODS

1. Animals

The current study was an experimental investigation carried out with permission from the Suez Canal University Faculty of Dentistry's Research Ethics Committee (REC), bearing approval number (403/2021).

The sample size was determined [8] with 30 samples each group and 10 samples per subgroup, the anticipated sample size was 60 samples total (n=60).

For this investigation, 60 female Sprague-Dawley rats weighing between 250 and 300 g and 6 months of age were acquired from Zagazig University's Faculty of Medicine. The rats were kept in suitable circumstances in cages and given water and soft food. Rats were randomly assigned into two major groups of thirty after a week of acclimation to the new laboratory conditions: an OVX group and a sham group.

2. Construction of the osteoporosis model

Ketamine-Xylazine (K: 75–90 mg/kg + X: 5–10 mg/kg in the same syringe) was injected intraperitoneally to anesthetize the animals before the surgery. Bilateral ovarian excision was carried out in the OVX group using the dorsal technique,

as previously reported[9]. Similar surgery was performed on the sham group, exposing the ovaries and reinstalling them in the same location without removing them.

2.3.Confirmation of the Success of Ovariectomy Procedure

The El-Borg laboratory's Zagazig branch's examination of the serum estradiol level (E2) confirmed the ovariectomy's effectiveness. It was conducted sixty days after the ovarian excision.

4. Preparation of the CTL-NE

CTL-NE preconcentrate was prepared by mixing 200 mg of CTL extract (Sigma-Aldrich, MO, USA) with purity greater than 98% with a mixture of 40% Capryol 90 (Gattefosse, Saint-Priest, France) and 60% Tween 80 (ADWIC Chemicals Co. Cairo, Egypt). The preconcentrate was diluted with purified water to generate nanoemulsions prior to the experiments.

5. The characterization techniques of CTL-NE:

- The size and shape of the generated CTL-NE were determined using transmission electron microscopy operated at a 200 kV accelerating voltage and connected to a Gatan camera at electron microscope unit, Faculty of Agriculture, Mansoura University.
- Zeta-potential measurements were made in a disposable cell using a Zeta sizer Nano ZS at electron microscope unit, Faculty of Agriculture, Mansoura University.

6. Characterization Results of the CTL-NE

6.1 Morphological analysis

Morphological analysis revealed homogenous spherical shaped particles. The size of developed dispersions was around 460 nm. Moreover, they were separated from each other without aggregation indicating effectiveness.

6.2 The zeta potential analysis (ZP)

The zeta potential detected for the synthesized CTL-NE was -60 mV. This highly negative zeta potential value reflects that the nanoemulsions possess high stability.

7. Animal subgrouping and drug administration

The rats of each group were further sectioned into 3 subgroups of 10 rats, the sham group was sectioned into: a) Subgroup 1.1 where the rats were left without any treatment, b) Subgroup 1.2 in which the animals received a daily dose of CTL (1.5mg/kg/day) orally by gavage for 4 weeks, c) Subgroup 1.3 where the rats were given a daily dose of CTL-NE (1.5mg/kg/day) orally by gavage for 4 weeks. While the OVX group was subdivided into: a) subgroup 2.1 in which the rats didn't have any treatment, b) subgroup 2.2 where the rats received a daily dose of CTL (1.5mg/kg/day) orally by gavage for 4 weeks similar to subgroup 1.2 and finally c) subgroup 2.3 where the rats were given a daily dose of CTL-NE (1.5mg/kg/day) orally by gavage for 4 weeks similar to subgroup 1.3 [10].

8. Euthanasia and sample collections

After finishing the treatment protocol for each group (4 weeks after osteoporosis confirmation), blood samples were collected for biochemical analysis of serum BTMs including alkaline phosphatase (ALP) and osteocalcin (OCN) then the rats were euthanized by overdose inhalation of Ether (Sigma-Aldrich, MO, USA) [11]. The lower jaw of each rat was dissected out, and their right halves were collected and immediately fixed with buffered formalin solution for histological examination.

9. Histological evaluation

After fixation, the specimens were decalcified in 5% formic acid. After complete decalcification, specimens were washed in distilled water, dehydrated in ascending grades of ethyl alcohol, cleared in xylene and embedded in paraffin. Serial sections (5μm) were cut and stained with hematoxylin and eosin (H&E) [12]. Afterward, the slides were visualized in a light microscope equipped with a built-in camera (OPTIKA Digital binocular brightfield microscope) at Histology department, Faculty of Medicine, Zagazig University.

10. Analysis of Plasma levels of ALP and OCN:

- They were measured at the research unit of Clinical Pathology Department, Zagazig University Hospital. Blood samples (2 ml) were collected in clean and dry Wasserman glass tubes from the right common carotid artery of each rat. They were left at room temperature for 30 minutes and then centrifuged at 300 rpm for 20 minutes.
- Serum was separated in 2 epindorf tubes:
- One sample for Quantitative determination of alkaline phosphatase according to manufacturer's instruction (Alkaline Phosphatase Sandwich ELISA Kit)
- Second sample for Quantitative measurements of Osteocalcin using Rat Osteocalcin ELISA kit.

Statistical Analysis

One-way ANOVA (analysis of variance) was used to conduct statistical analyses of BTMs. The statistical significance between the subgroups was assessed using Tukey's post hoc test. A P value of less than 0.05 is regarded as statistically significant. Version 22.0 of the SPSS software for Windows (Statistical Package for Social Science, Armonk, NY: IBM Corp.) was used to conduct the analysis.

RESULTS

Osteoporosis induction confirmation

The induction of osteoporosis was confirmed by analysis of serum E2 level. Rats of the sham group showed mean E2 of 77.57 U/L. while OVX rats displayed mean E2 of 21.86 U/L.

Histological results

- In the sham group, subgroup 1.1 showed normal bone architecture of the mandibular bone formed of cortical compact bone and supporting spongy bone. Cortical compact bone made of "osteons" had closely packed bone lamellae surrounding the central Haversian canal. The osteocytes in their lacunae were found between these bone lamellae (fig1. A). while spongy bone was composed of dense connected bone trabeculae containing osteocytes trapped within their lacunae. These trabeculae enclosing marrow cavities that contain bone marrow and lined by endosteum (fig2. A).
- Subgroup 1.2 (fig1. B & fig2. B) and subgroup 1.3 (fig1. C & fig2. C) showed normal histological mandibular bone appearance formed of cortical bone with compacted bone lamellae and its supporting spongiosa like that of subgroup 1.1.
- In the OVX group, the histological examination of subgroup 2.1 mandibular bone exhibited clear morphological alterations. The cortical bone plate had loosely arranged lamellae (fig1. D). Also, supporting bone characterized by sparse bone trabeculae with loss of trabecular connectivity and widening of inter-trabecular spaces. Moreover, the wide marrow cavities were associated with fatty tissue infiltration and eroded scalloped margin. Degeneration of

osteocytes and absence of osteoblastic lining could also be noticed (fig2. D).

- Light microscopic examination of subgroup 2.2 showed notable improvement regarding bone architecture compared with subgroup 2.1 as the cortical compact bone regained the appearance of closely packed bone lamellae (fig1. E). However, the widening of inter-trabecular spaces and loss of connectivity in spongy bone were still notable (fig2. E).
- Histological examination of subgroup 2.3 showed that the bone almost had normal microstructure. The compact bone had closely packed bone lamellae (fig1. F). the supporting bone almost recovered its normal architecture of thick connecting bone trabeculae (fig2. F).

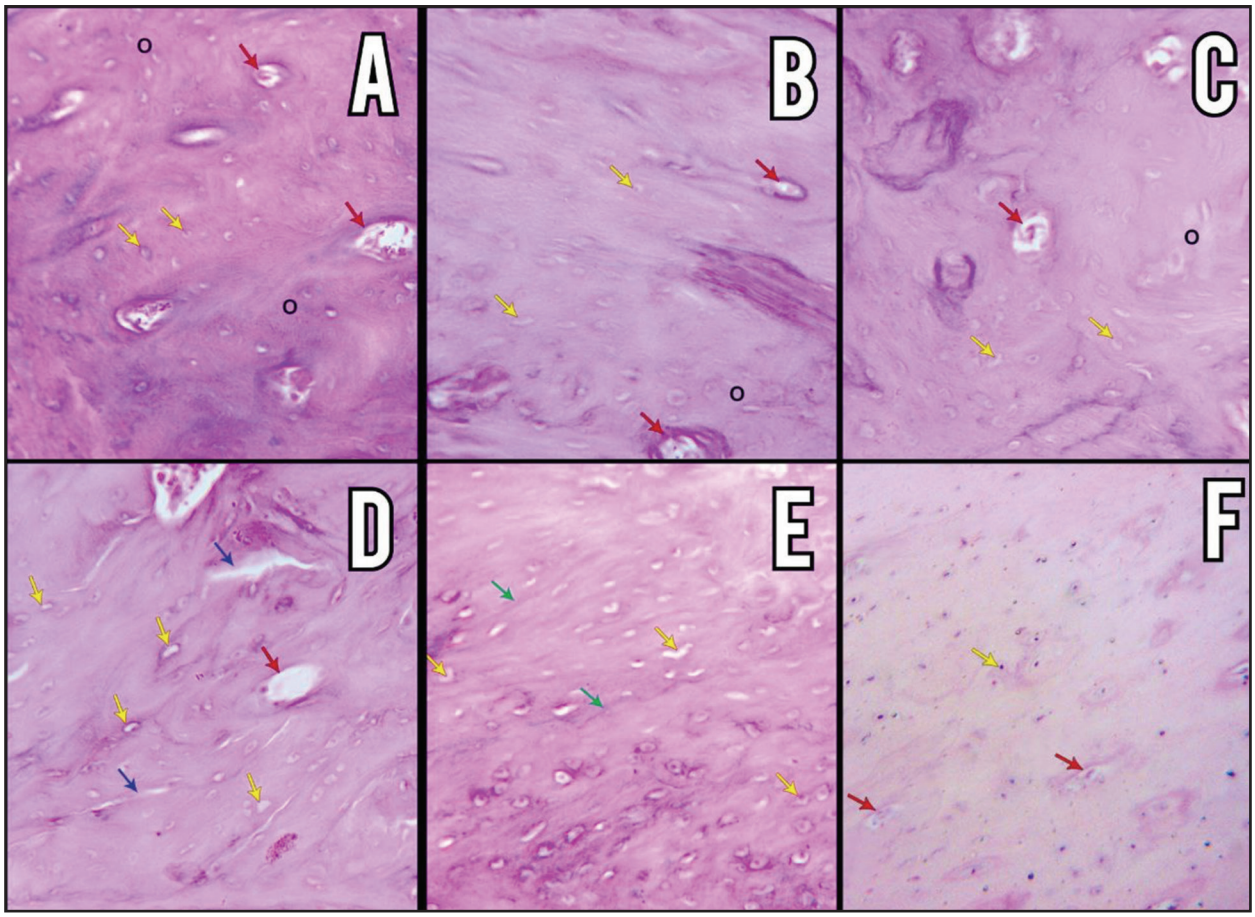

Fig. (1) Light micrographs of the mandibular cortical bone in (A) subgroup 1.1 showing normal osteons (O) formed of concentric bone lamellae & Haversian canal (red arrow). (B) subgroup 1.2 with normal cortical bone appearance where the osteocytes are arranged among the closely packed bone lamellae (yellow arrow). (C) cortical bone of subgroup 1.3. (D) showing subgroup 2.1 with abnormal osteons architecture with the bone lamellae separated from each other (blue arrow) and some osteocytes lacunae were empty (yellow arrow). Note that the Haversian canals were devoid of their contents (red arrow). (E) the compact bone of subgroup 2.2 started to regain the appearance of closely packed bone lamellae and Osteocytes of variable shape and size had irregular arrangement within the lamellae (yellow arrow). (F) subgroup 2.3 cortical bone almost regained its normal compact appearance with centrally situated haversian canal (red arrow). Note the regular distribution of osteocytes appeared of almost normal shape and small size (yellow arrow). (H&E Orig. mag. X200)

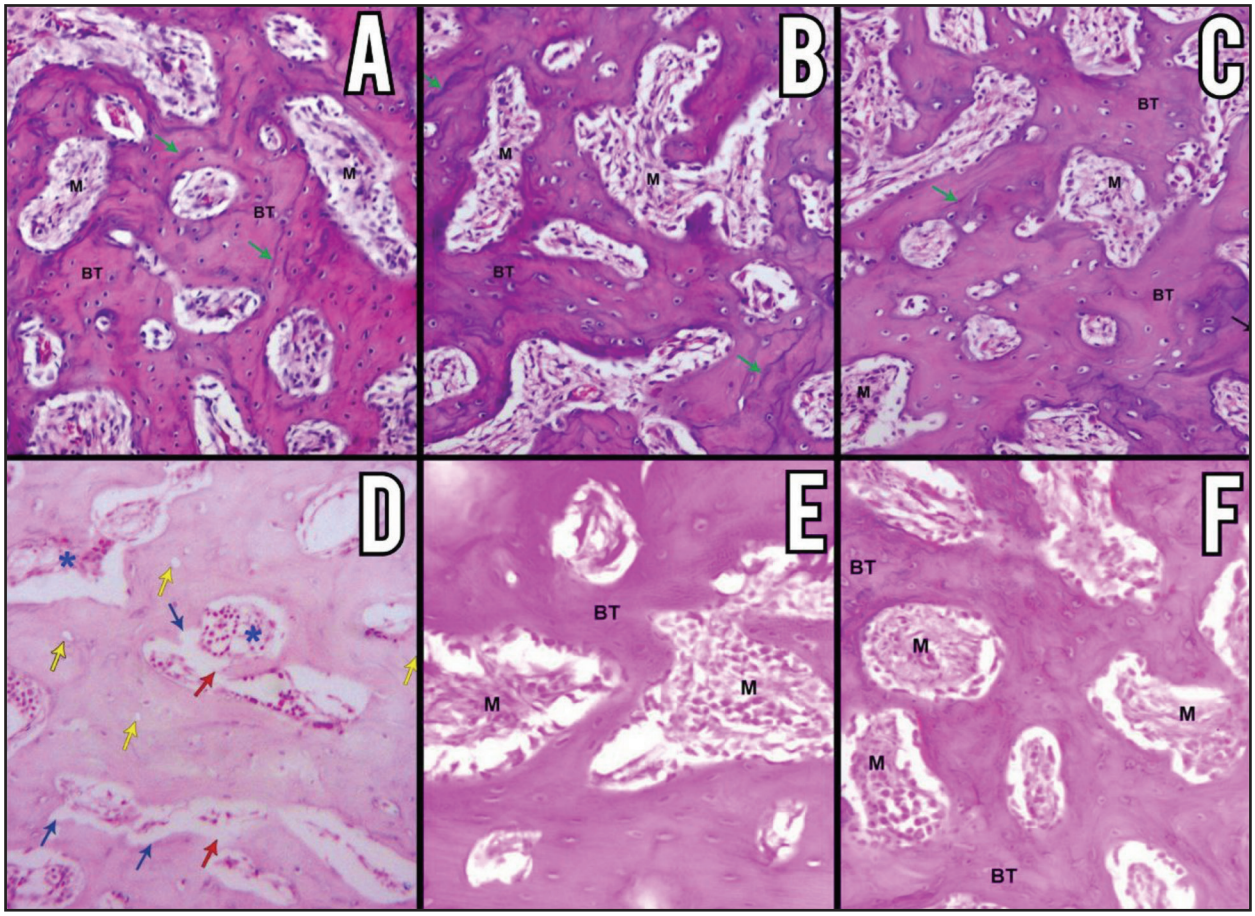

Fig. (2) Light micrographs of the mandibular spongy bone in (A) where subgroup 1.1 showed normal supporting bone composed of thick bone trabeculae (BT) surrounding the marrow spaces (M). (B) subgroup 1.2 composed of dense bone trabeculae (BT) surrounding the irregular medullary spaces (M). In (C) had also spongy bones of normal appearance. In (D) subgroup 2.1 1spongiosa showed loss of trabecular connectivity (red arrow). The wide trabecular spaces had numerous fat vacuoles (*) and presented scalloped irregular margin (blue arrow). Note the empty osteocyte lacunae dispersed within the bone trabeculae (yellow arrow). (E) showed subgroup 2.2 with thin bone trabeculae (BT) and numerous wide medullary spaces of large size (M). (F) where subgroup 2.3 exhibited marked improvement in bone architecture having thick bone trabeculae (BT) with osteocytes trapped in their lacunae and numerous irregular medullary spaces (M). (H&E Orig. mag. X200)

Biochemical Evaluation:

A. Serum ALP levels

Analysis of serum ALP mean values demonstrated clearly significant difference between the studied groups. In sham subgroups, subgroup 1.2 recorded 124.00 U/L mean value for ALP which was significantly higher than that recorded in subgroup 1.3 which was 100.00 U/L and lower than that of subgroup 1.1 which was165.00U/L. while in OVX subgroups, subgroup 2.2 recorded 326.67 U/L mean value for ALP which was significantly higher than ALP level in subgroup 2.3 that was 180.00U/L and lower levels than that recorded in subgroup 2.1 which was 394.00 U/L (Table1).

Table (1) *The mean and standard deviation of ALP among the studied subgroups.*

Subgroup	Mean	SD	F	P value
Subgroup 1.1	165.00[d]	9.88	1255.76	<0.001**
Subgroup 1.2	124.00[e]	13.08		
Subgroup 1.3	100.00[f]	5.37		
Subgroup 2.1	394.00[a]	6.03		
Subgroup 2.2	326.67[b]	5.05		
Subgroup 2.3	180.00[c]	6.36		

*** and different superscript letters mean significant at P<0.005*

B. Serum OCN levels

The study of serum OCN mean levels showed also significant difference between the various groups. In sham subgroups, subgroup 1.2 recorded 12.93ng/ML mean value for OCN which was significantly higher than that recorded in subgroup 1.3 which was 11.83 ng/ML and lower than that of subgroup 1.1 which was 16.50 ng/ML. whereas in OVX subgroups, subgroup 2.2 recorded 31.0ng/ML mean value for OCN which was significantly higher than OCN level in subgroup 2.3 that was 17.0ng/ML and lower levels than that of subgroup 2.1 which was 42.48 ng/ML (Table2).

Table (2) *The mean and standard deviation of osteocalcin among the studied subgroups.*

Subgroups	Mean	SD	F	P value
Subgroup 1.1	16.50[c]	1.05	748.54	<0.001**
Subgroup 1.2	12.93[d]	0.20		
Subgroup 1.3	11.83[d]	0.41		
Subgroup 2.1	42.48[a]	1.62		
Subgroup 2.2	31.00[b]	0.89		
Subgroup 2.3	17.00[c]	1.55		

*** and different superscript letters mean significant at P<0.005*

DISCUSSION

The present study attempted to address two research points. First, the effects of PMOP on the mandibular bone microstructure. The second, the osteoprotective proficiency of CTL and CTL-NE as an emerging nutraceutical.

The most widely used and established technique for creating artificial PMOP in rats is the OVX rat model [13], and mandibular osteoporosis is thought to be a localized expression of this general osteoporosis in the oral and maxillofacial regions as many researchers found that the mandibular bone has the fastest turnover rate, and mandibular bone loss may represent the first sign of osteoporosis [14].

The results of the present investigation highlighted qualitatively, using L.M, and quantitatively, using biochemical analysis of BTMs, the destructive effects of OVX on mandibular bone architecture. It is imperative to recall that PMOP and osteoporosis-like changes in OVX not only associated with hormonal changes "estrogen deficiency" that upregulates bone resorption by increasing osteoclast formation and prolonging their lifespan, but also other factors are involved in their pathogenesis, including aging, oxidative stress, and inflammation [15,16].

In the current study, the loosely arranged lamellae detected in the cortical plate came in accordance with the data reported by **Xiong *et al.*** [17]. They brought that back to the impaired OPG/RANKL/RANK signaling pathway under estrogen deficiency conditions. Moreover, **Guo *et al.*** noticed that the trabecular network was less dense and irregular in OVX specimens compared to sham ones [18]. While the study conducted by **Huang *et al***. confirmed the increased bone marrow adiposity in OVX rats and attributed that to the increased adipogenic differentiation capacity related to age that eventually leads to osteoporosis [19].

The changes in bone cellularity observed in L.M examinations came in line with the results informed by Mohamad et al. who confirmed the presence of empty osteocytes lacunae and eroded bone surface in OVX rats [20]. Moreover, A similar study, conducted by Salih and AL-Khashab on rat femur bone, reported a low number of osteoblasts, in addition to high numbers of osteoclasts in the OVX group [21].

Osteocyte apoptosis is associated with increased bone resorption due to signaling neighboring cells to express RANKL or independently by releasing apoptotic bodies, which recruit osteoclast precursors. Additionally, apoptotic osteocytes undergo secondary necrosis due to their position in bone, which prevents their phagocytosis, and this is accompanied by the release of damage-associated molecular patterns (DAMPs), that activate the monocytic release of inflammatory cytokines and amplify osteoclastogenic signals. Besides, senescent osteocytes acquire SASP accompanied with increased RANKL expression, and decreased Wnt16 expression [22].

In the present study, rats of OVX subgroup 2.1 exhibited significant increase of their serum ALP and OCN levels above that of the sham 1.1 subgroup. These results verified the effectiveness of OVX rat model used in the current study in creating estrogen deficient condition resembling that existed in PMOP. Moreover, these findings came in agreement with others that confirmed a strong negative relation between BTMs and bone mineral density (BMD) under estrogen deficient condition and it's attributed to the increase in bone turnover rate related to age [23].

Interestingly, the present work highlighted the osteoprotective efficiency of CTL and CTL-NE by preserving almost normal bone architecture under estrogen deficient condition. Like our study, **Xu *et al***. demonstrated that CTL reduced bone loss in the OVX-induced osteoporosis model by suppressing the NF-ϰB and MAPK signaling pathways mediated by Transforming Growth Factor β-activated kinase 1 (TAK1), which in turn inhibited osteoclast production and activity [24].

Many studies introduced CTL as a promising antioxidant, anti-inflammatory and immunomodulatory nutraceutical agent. CTL can activate the AMPK/SIRT1-PGC-1α signaling pathway that exerts an urgent function in defending against ROS accumulation in osteoporosis and aging. Moreover, it downregulates the synthesis of pre-inflammatory cytokines and chemokine (IL-1α, IL-6 and MCP-1) indicating that it exerts anti-inflammatory activity[25]. Likewise, a study conducted by Zeng et al. reported that CTL exerted immunomodulatory functions by regulating PI3K/AKT signaling pathway, T17 cell differentiation, MAPK signaling pathway, TNF signaling pathway, TGF-β/SMAD signaling pathway, IL-17 signaling pathway, JAK-STAT signaling pathway and other major signaling pathways by acting on key targets such as TNF and IL6 [26].

In the current study, the efficacy of CTL was also confirmed quantitatively by analyzing BTMs. Rats of OVX group that received a daily dose of CTL were found to have marked decrease in serum levels of ALP and OCN compared with their counterpart that didn't receive any treatment suggesting a shift in bone remodeling in favor of an anti-osteoclastic activity. Similarly, **Xi *et al***. observed that CTL reduced ALP and OCN expression levels in glucocorticoid-induced osteoporotic rats (GIOP)[27]. Furthermore, Liu et al. reported a decrease in serum ALP concentration in a mouse model of secondary osteoporosis upon CTL administration and attributed that to the ameliorative effect of CTL on abnormal bone metabolism [28].

Interestingly, incorporating CTL into nanoemulsion boosts its osteoprotective capacity. This is confirmed qualitatively by the enhanced bone microstructure picture under L.M and quantitatively by the decrease in serum BTMs levels in CTL-NE treated OVX rats compared with the CTL treated ones. Similarly, **Zhou *et al.*** proved that CTL therapeutic abilities were strengthened after being formed into nanodrugs [29].

Many other studies established the efficacy of CTL nanoformulations in enhancing the therapeutic activities while offering promising safety in comparison with traditional formulations and attributed that to (i) improved drug solubility and oral bioavailability, (ii) prolonged blood circulation times through better protection before reaching the targeting sites and (iii) targeted drug delivery to improve drug efficacy and reduce systemic toxicity[30-32].

CONCLUSION

The osteoprotective effects of CTL can be augmented by incorporating it into nanoemulsion formulations.

REFERENCES

1. Geraci A, Calvani R, Ferri E, Marzetti E, Arosio B, Cesari M. Sarcopenia and menopause: the role of estradiol. Front Endocrinol. 2021; 12: 682012.
2. Song S, Guo Y, Yang Y, Fu D. Advances in pathogenesis and therapeutic strategies for osteoporosis. Pharmacol Ther. 2022; 237:108168.
3. Słupski W, Jawień P, Nowak B. Botanicals in postmenopausal osteoporosis. Nutr. 2021; 13(5): 1609.
4. Shan Y, Zhao J, Wei K, Jiang P, Xu L, et al. A comprehensive review of Tripterygium wilfordii hook. f. in the treatment of rheumatic and autoimmune diseases: bioactive compounds, mechanisms of action, and future directions. Front pharmacol. 2023; 14: 1282610.
5. Shi J, Li J, Xu Z, Chen L, Luo R, et al. Celastrol: A Review of Useful Strategies Overcoming its Limitation in Anticancer Application. Front Pharmacol. 2020; 11: 11.
6. Wagh PR, Desai P, Prabhu S, Wang J. Nanotechnology-based celastrol formulations and their therapeutic applications. Front pharmacol. 2021; 12: 673209.
7. Qiu N, Liu Y, Liu Q, Chen Y, Shen L, et al. Celastrol nanoemulsion induces immunogenicity and downregulates PD-L1 to boost abscopal effect in melanoma therapy. Biomater. 2021; 269:120604.
8. Charan J, Biswas T. (2013). How to calculate sample size for different study designs in medical research?. Indian J Psychol Med. 2013; 35(2): 121-126.
9. Ponnusamy V, Solaiyappan K, Govindarasu M, Prathap L, Babu S, et al. Effect of estradiol on histopathology of brain in unilateral and bilateral ovariectomized rats. Bioinformation. 2023; 19(6):703.
10. Nie Y, Fu C, Zhang H, Zhang M, Xie H, et al. Celastrol slows the progression of early diabetic nephropathy in rats via the PI3K/AKT pathway. BMC complement med ther. 2020; 20:1-14.
11. Suckow M, Gimpel J. Approaches to the humane euthanasia of research animals. Anim Biotechnol. 2020; 731: 3.
12. Emara RS, Noya DE. Comparative histological study on the possible protective effect of Mitoquinone versus Oxymatrine on cerebellar cortex of adult male albino rats treated with Sofosbuvir. EJH.3:23;2024 .
13. Yousefzadeh N, Kashfi K, Jeddi S, Ghasemi A. Ovariectomized rat model of osteoporosis: a practical guide. EXCLI journal. 2020; 19: 89.
14. Jonasson G, Skoglund I, Rythén M. The rise and fall of the alveolar process: Dependency of teeth and metabolic aspects. Arch Oral Biol. 2018; 96: 195.
15. Shahriarpour Z, Nasrabadi B, Hejri-Zarifi S, Shariati-Bafghi SE, Yousefian-Sanny M, et al. Oxidative balance score and risk of osteoporosis among postmenopausal Iranian women. Arch Osteoporos. 2021; 16: 1.
16. Wu D, Cline-Smith A, Shashkova E, Perla A, Katyal A, et al. T-cell mediated inflammation in postmenopausal osteoporosis. Front Immunol. 2021; 12: 687551.

17. Haffner-Luntzer M, Fischer V, Prystaz K, Liedert A, Ignatius A. The inflammatory phase of fracture healing is influenced by oestrogen status in mice. Eur J Med Res. 2017; 22: 1.

18. GuoX, Yu X, Yao Q, QinJ. Early effects of ovariectomy on bone microstructure, bone turnover markers and mechanical properties in rats. BMC Musculoskelet Disord. 2022;23(1):316.

19. Huang L, Lu S, Bian M, Wang J, et al. (2023). Punicalagin attenuates TNF-α-induced oxidative damage and promotes osteogenic differentiation of bone mesenchymal stem cells by activating the Nrf2/HO-1 pathway. Exp Cell Res. 2023; 430(1):113717.

20. Mohamad N, Ima-Nirwana S, Chin K. Self-emulsified annatto tocotrienol improves bone histomorphometric parameters in a rat model of oestrogen deficiency through suppression of skeletal sclerostin level and RANKL/OPG ratio. Int J Med Sci. 2021;18(16): 3665.

21. Salih S, AL-Khashab E. Effect of atorvastatin on bone formation in ovariectomized rats. IJVS.2023; 37(1):239.

22. McCutcheon S, Majeska R, Spray D, Schaffler M, Vazquez M. Apoptotic osteocytes induce RANKL production in bystanders via purinergic signaling and activation of pannexin channels. JBMR. 2020; 35(5): pp.966.

23. Hsu C, Ko P, Kwan T, Liu M, Jou I, et al. Daily supplement of sesame oil prevents postmenopausal osteoporosis via maintaining serum estrogen and aromatase levels in rats. Sci Rep. 2024;14(1): 321.

24. Xu Q, Chen G, Xu H, Xia G, Zhu M, et al. Celastrol attenuates RANKL-induced osteoclastogenesis in vitro and reduces titanium particle-induced osteolysis and ovariectomy-induced bone loss in vivo. Front Pharmacol. 2021; 12: 682541.

25. Li L, Wang B, Li Y, Li L, Dai Y, et al. Celastrol regulates bone marrow mesenchymal stem cell fate and bone-fat balance in osteoporosis and skeletal aging by inducing PGC-1α signaling. Aging. 2020;12(17):6887.

26. Zeng L, Yu G, Yang K, He Q, Hao W, et al. Exploring the mechanism of Celastrol in the treatment of rheumatoid arthritis based on systems pharmacology and multi-omics. Sci Rep. 2024; 14(1):1604.

27. Xi J, Li Q, Luo X, Wang Y, Li J, et al. Celastrol inhibits glucocorticoid induced osteoporosis in rat via the PI3K/AKT and Wnt signaling pathways. Mol Med Rep. 2018; 18(5):4753.

28. Liu X, Cai F, Zhang Y, Yang A, Liu L. Celastrol, an NF-κB inhibitor, ameliorates hypercalciuria and articular cartilage lesions in a mouse model of secondary osteoporosis. J Pharmacol Sci. 2016; 130(4):204.

29. Zhou M, Liao J, Lai W, Xu R, Liu W, et al. A celastrol-based nanodrug with reduced hepatotoxicity for primary and metastatic cancer treatment. EBioMedicine. 2023; 94:322.

30. Guo L, Zhang Y, Al-Jamal KT. Recent progress in nanotechnology-based drug carriers for celastrol delivery. Biomaterials Science. 2021; 9(19):6355.

31. Wagh P R, Desai P, Prabhu S, Wang J. Nanotechnology-based celastrol formulations and their therapeutic applications. Front Pharmacol. 2021; 12: 673209.

32. Fang G, Tang B. Current advances in the nano-delivery of celastrol for treating inflammation-associated diseases. J Mater Chem B. 2020; 8(48):10954.